Supplementary Information (SI) for Journal of Materials Chemistry A.
This journal is © The Royal Society of Chemistry 2024

Supporting Information

Cu doping as electron buffers for stabilizing Ru-based active layers for hydrogen evolution

Xinyu Wang[a, b], *Tongtong Liu*[*a, d], *Jingjing Wang*[c], *Bowen Xia*[c], *Yanfei Wang*[*c], *Zhilin Li*[a, b], *Zhengping Zhang*[*a, b], *Feng Wang*[*a, b]

a. State Key Laboratory of Chemical Resource Engineering, Beijing Key Laboratory of Electrochemical Process and Technology for Materials, Beijing University of Chemical Technology, Beijing 100029, P. R. China.

b. National Engineering Research Center for Fuel Cell and Hydrogen Source Technology, Beijing University of Chemical Technology, Beijing 100029, P. R. China.

c. Petrochina Petrochemical Research Institute, Beijing 102206, P. R. China

d. Beijing Huairou Laboratory, Beijing 101400, P. R. China

*Corresponding author: zhangzhengping@mail.buct.edu.cn; wangf@mail.buct.edu.cn; liutongt0374@163.com (T. L); wangyanfei010@petrochina.com.cn (Y. Wang)

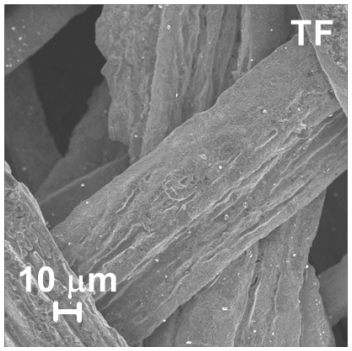

Figure S1. SEM images of Ti fiber felt.

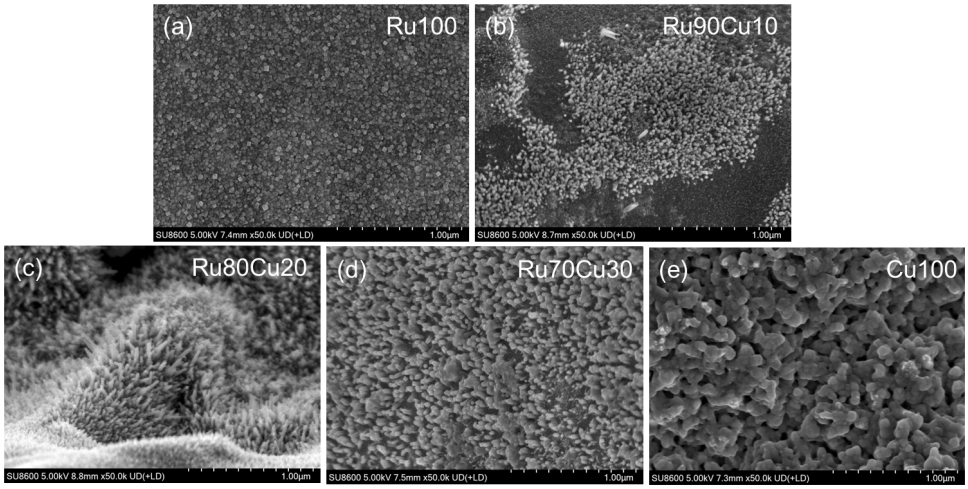

Figure S2. SEM images of (a) $Ru_{100}Cu_0$/TF (RuO_2/TF), (b) $Ru_{90}Cu_{10}$/TF, (c) $Ru_{80}Cu_{20}$/TF (RCO/TF), (d) $Ru_{70}Cu_{30}$/TF and (e) Ru_0Cu_{100}/TF (CuO/TF).

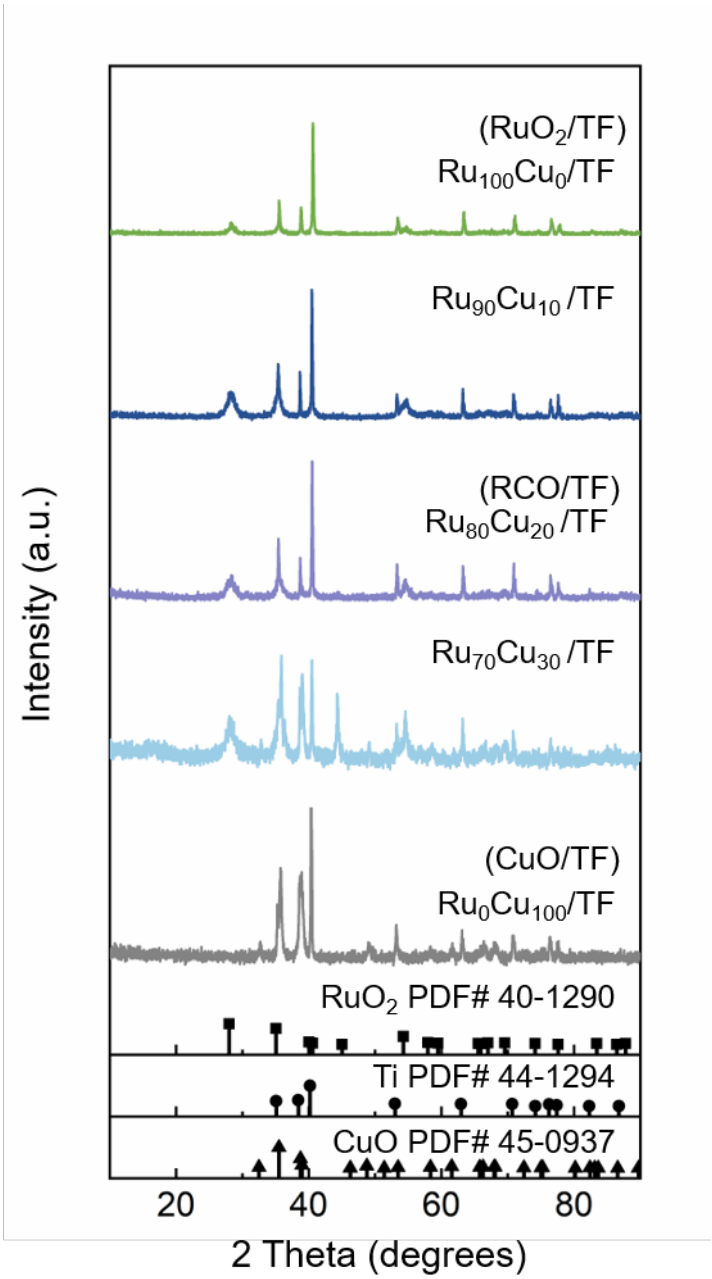

Figure S3. The XRD patterns of $Ru_{100}Cu_0$/TF (RuO_2/TF), $Ru_{90}Cu_{10}$/TF, $Ru_{80}Cu_{20}$/TF (RCO/TF), $Ru_{70}Cu_{30}$/TF and Ru_0Cu_{100}/TF (CuO/TF).

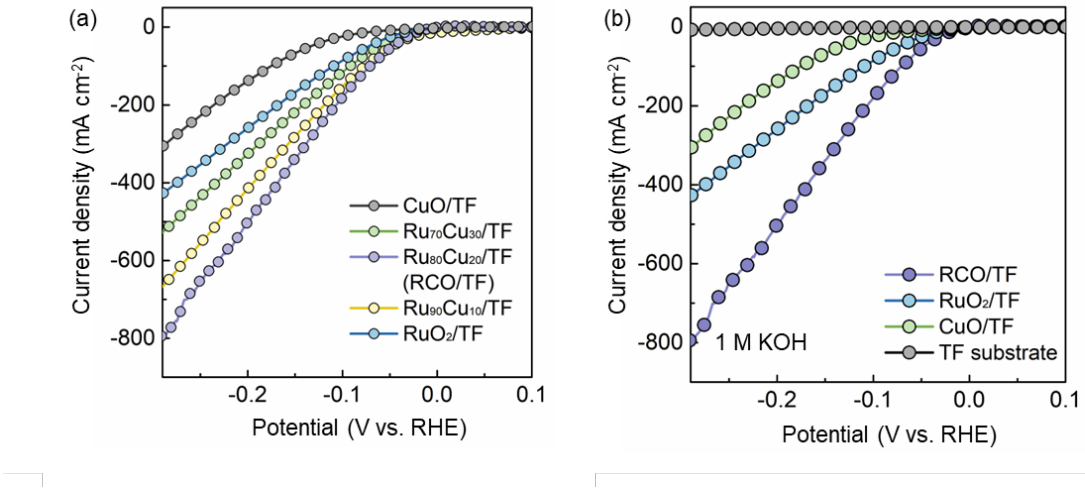

Figure S4. (a) The LSV curves recorded at a scan rate of 10 mV s^{-1} in 1 M KOH solution for $Ru_{100}Cu_0$/TF (RuO_2/TF), $Ru_{90}Cu_{10}$/TF, $Ru_{80}Cu_{20}$/TF (RCO/TF), $Ru_{70}Cu_{30}$/TF and Ru_0Cu_{100}/TF (CuO/TF). (b) The LSV curves recorded at a scan rate of 10 mV s^{-1} in 1 M KOH solution for RCO/TF, RuO_2/TF, CuO/TF and TF.

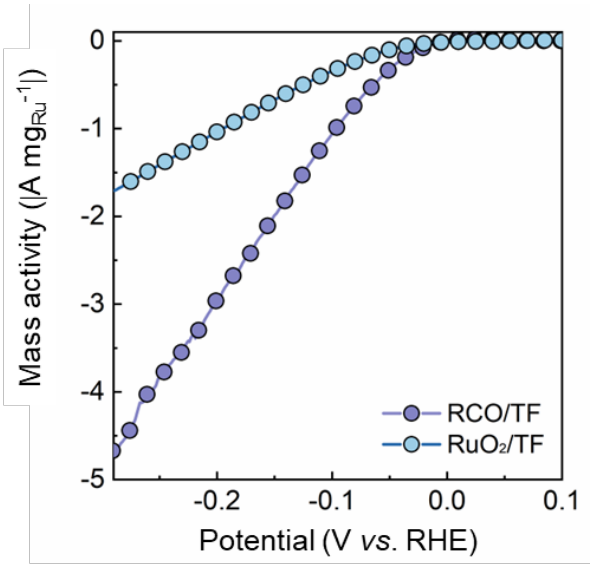

Figure S5. The mass activity comparison of RCO/TF and RuO_2/TF.

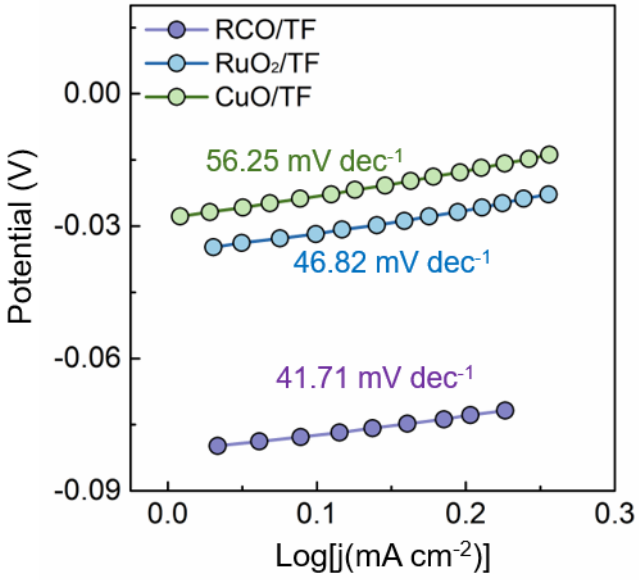

Figure S6. Tafel plots derived from the LSV curves for RCO/TF, RuO_2/TF and CuO/TF.

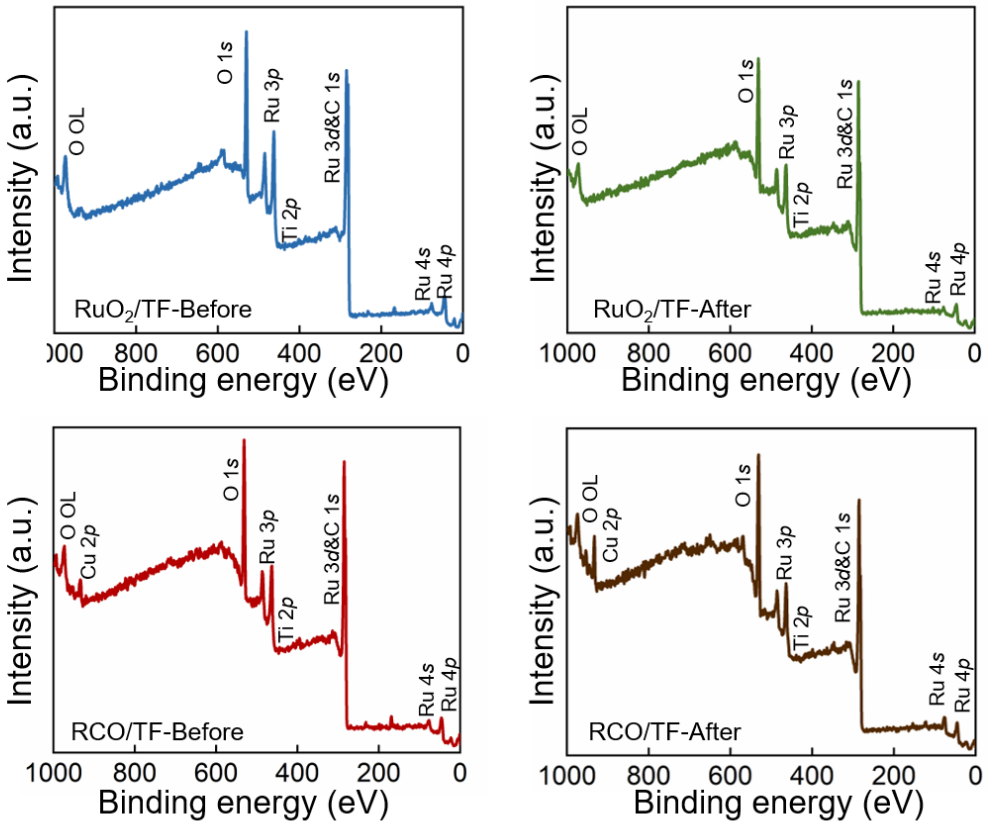

Figure S7. XPS survey spectra for (a) RuO_2/TF, (b) RuO_2/TF-after reaction, (c) RCO/TF and (d) RCO/TF-after reaction.

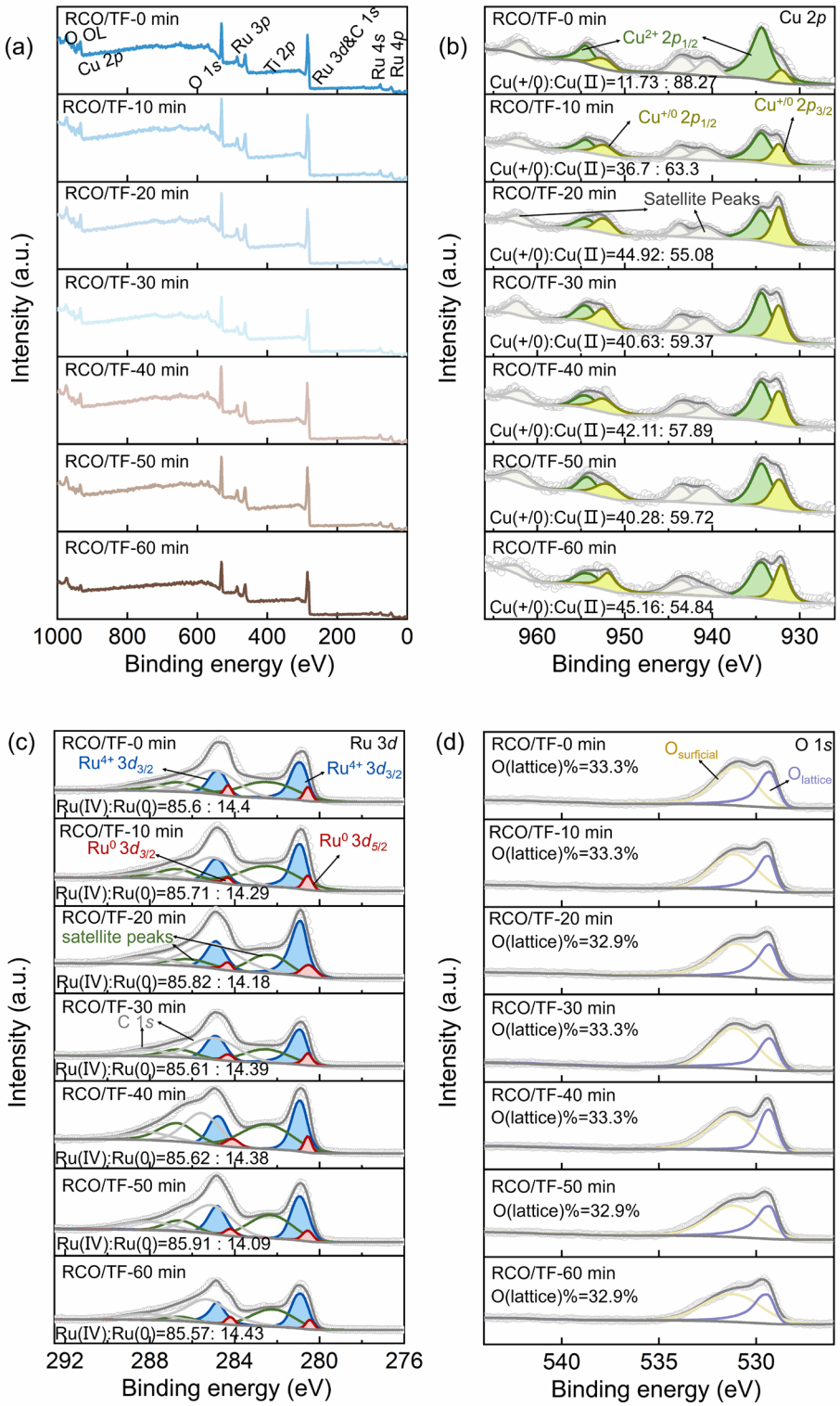

Figure S8. (a) XPS survey spectra, (b) High-resolution Cu 2*p* XPS spectra, (c) High-resolution Ru 3*d* XPS spectra and (d) High-resolution O 1*s* spectra of RCO/TF-0 min, -10 min, -20 min, -30 min, -40 min, -50 min, -60 min.

.

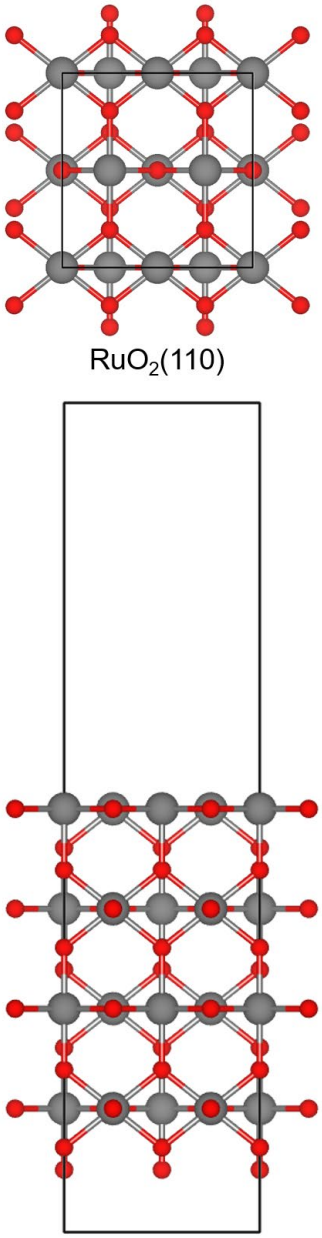

Figure S9. The configuration of $RuO_2(110)$ model.

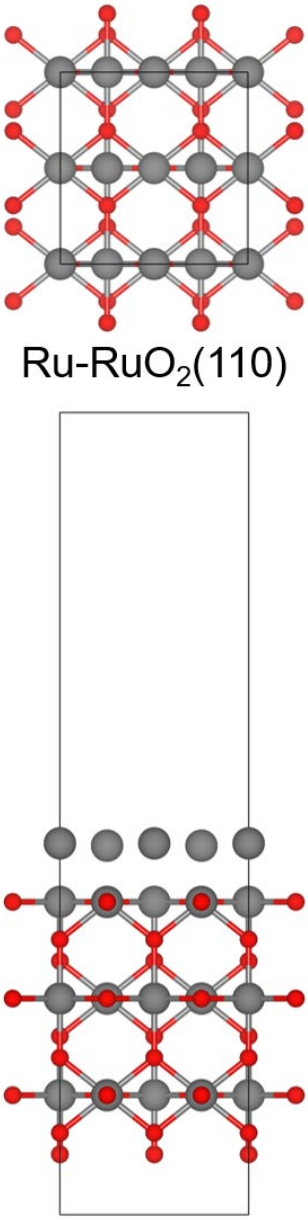

Figure S10. The configuration of Ru-RuO_2(110) model.

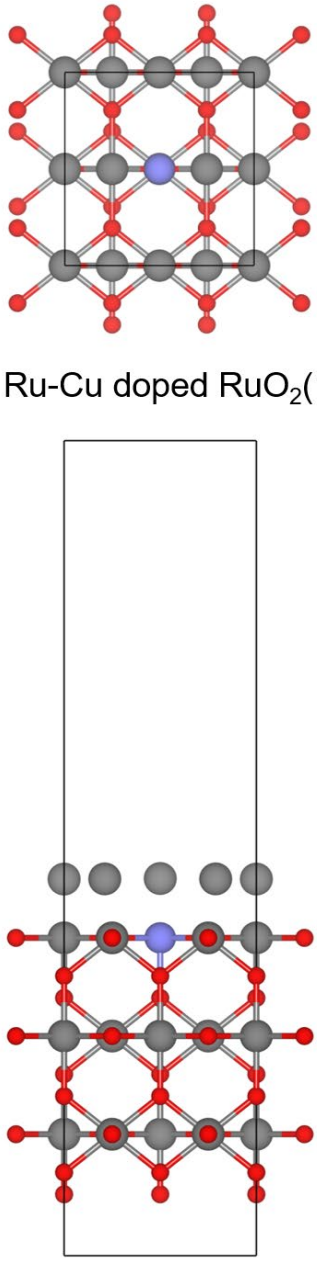

Figure S11. The configuration of Ru-Cu doped RuO_2(110) model.

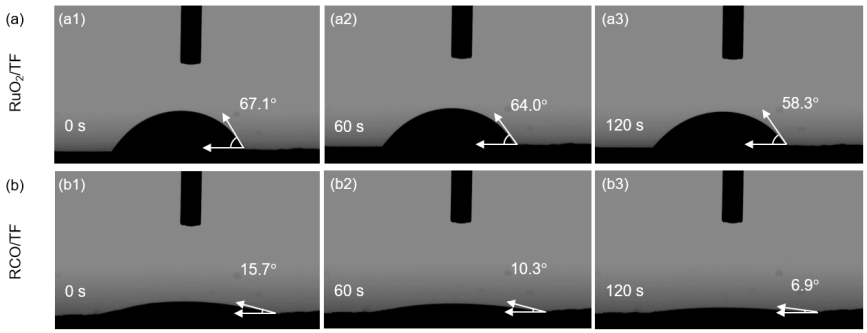

Figure S12. (a1) - (a3) The wetting ability tests of RuO_2/TF, and (b1) - (b3) those of RCO/TF.

Table S1. Current efficiencies corresponding to RCO/TF||Ni and RuO_2/TF||Ni for current densities of 0.1 A/cm^2 and 1 A/cm^2, respectively.

	0.1 A/cm^2	1 A/cm^2
RCO/TF||Ni	95.24%	95.25%
RuO_2/TF||Ni	86.95%	80.97%

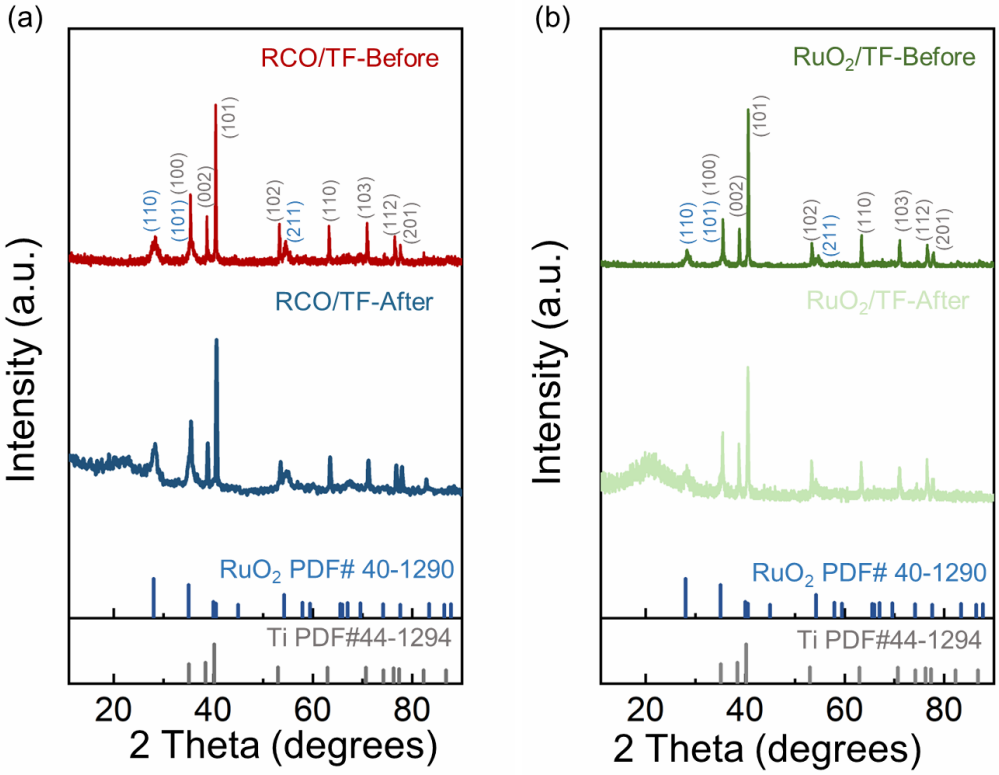

Figure S13. The XRD patterns of (a) RCO/TF and (b) RuO_2/TF before and after AWE operation.

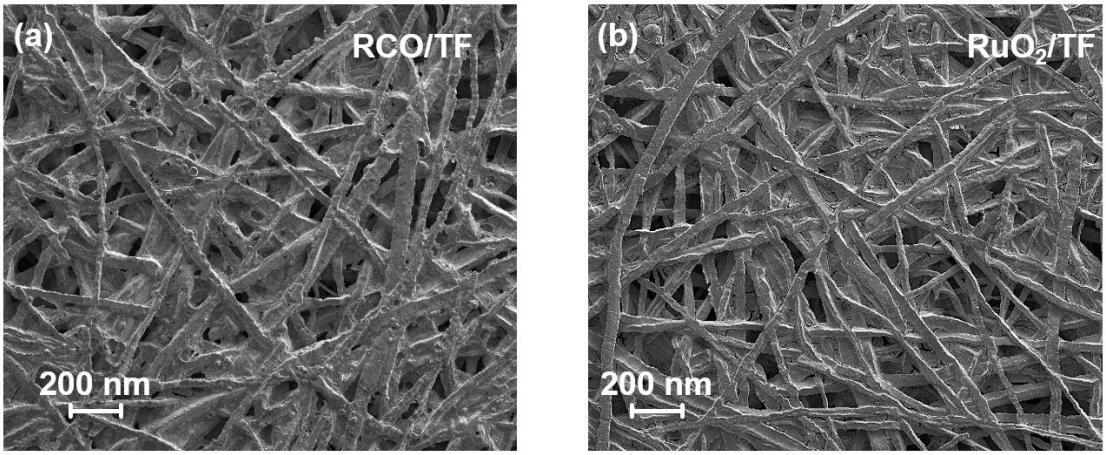

Figure S14. SEM images of (a) RCO/TF and (b) RuO_2/TF before AWE operation.

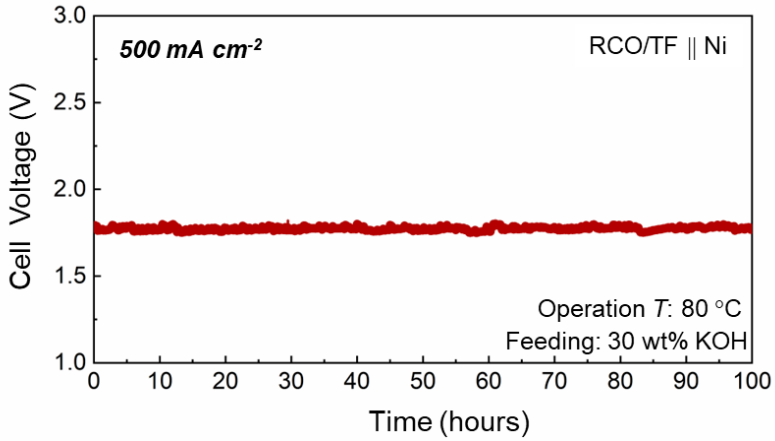

Figure S15. The typical galvanostatic curves of the as-assembled AEM electrolyzer (Ni foam as the anode and RCO/TF as the cathode) at 500 mA cm^{-2} during the overall water splitting.